

# Life history, larval dispersal, and connectivity in coral reef fish among the Scattered Islands of the Mozambique Channel

James L. O'Donnell<sup>1,4</sup> · Ricardo Beldade<sup>2,3</sup> · Suzanne C. Mills<sup>2,3</sup> · Hannah E. Williams<sup>1</sup> · Giacomo Bernardi<sup>1</sup>

Received: 3 February 2016 / Accepted: 23 August 2016 / Published online: 7 September 2016  
© Springer-Verlag Berlin Heidelberg 2016

**Abstract** The Western Indian Ocean harbors one of the world's most diverse marine biota yet is threatened by exploitation with few conservation measures in place. Primary candidates for conservation in the region are the Scattered Islands (Îles Éparses), a group of relatively pristine and uninhabited islands in the Mozambique Channel. However, while optimal conservation strategies depend on the degree of population connectivity among spatially isolated habitats, very few studies have been conducted in the area. Here, we use highly variable microsatellite markers from two damselfishes (*Amphiprion akallopisos* and *Dascyllus trimaculatus*) with differing life history traits [pelagic larval duration (PLD), adult habitat] to compare genetic structure and connectivity among these islands using classic population structure indices as well as Bayesian clustering methods. All classical fixation indexes

$F_{ST}$ ,  $R_{ST}$ ,  $G'_{ST}$ , and Jost's  $D$  show stronger genetic differentiation among islands for *A. akallopisos* compared to *D. trimaculatus*, consistent with the former species' shorter PLD and stronger adult site attachment, which may restrict larval dispersal potential. In agreement with these results, the Bayesian analysis revealed clear genetic differentiation among the islands in *A. akallopisos*, separating the southern group (Bassas da India and Europa) from the center (Juan de Nova) and northern (Îles Glorieuses) islands, but not for *D. trimaculatus*. Local oceanographic patterns such as eddies that occur along the Mozambique Channel appear to parallel the results reported for *A. akallopisos*, but such features seem to have little effect on the genetic differentiation of *D. trimaculatus*. The contrasting patterns of genetic differentiation between species within the same family highlight the importance of accounting for diverse life history traits when assessing community-wide connectivity, an increasingly common consideration in conservation planning.

James L. O'Donnell and Ricardo Beldade have contributed equally to this work.

Communicated by Ecology Editor Dr. Michael Berumen

**Electronic supplementary material** The online version of this article (doi:10.1007/s00338-016-1495-z) contains supplementary material, which is available to authorized users.

✉ James L. O'Donnell  
jodonnellbio@gmail.com

<sup>1</sup> Department of Ecology and Evolutionary Biology, University of California, Santa Cruz, CA 95060, USA

<sup>2</sup> EPHE, PSL Research University, UPVD-CNRS, USR 3278, CRILOBE, 98729 Papetoai-Moorea, French Polynesia

<sup>3</sup> Laboratoire d'Excellence «CORAIL», Moorea, France

<sup>4</sup> Present Address: School of Marine and Environmental Affairs, University of Washington, Seattle, WA 98105, USA

**Keywords** Population genetics · Population structure · *Amphiprion akallopisos* · *Dascyllus trimaculatus* · Pomacentridae · Îles Éparses

## Introduction

The Western Indian Ocean is one of the most biodiverse yet understudied regions of the sea (McClanahan et al. 2000; Roberts et al. 2002). In addition to high levels of local diversity and endemism, there is substantial turnover in species composition between this region and the epicenter of marine biodiversity, the Coral Triangle (Allen 2008; Briggs and Bowen 2012; Obura 2012, 2015). These attributes make the Western Indian Ocean an important

priority for conservation, yet presently its coral reefs are afforded little protection from exploitation (Mora et al. 2006). Human populations in this region are growing rapidly, increasingly relying on marine organisms as a food source and as an economic resource. The combined threat of global climate change (McClanahan et al. 2014; Mills et al. 2015) and anthropogenic disturbances has generated growing interest in creating reserves that will help sustain populations of marine organisms both for their economic and intrinsic values. Optimization of the size, spatial arrangement, and management of ecological reserves so that they effectively serve their intended purpose requires an understanding of the movement of individuals among populations in the area of interest (Halpern and Warner 2003).

The majority of marine organisms exhibit a bipartite life history, where adults are sedentary and larvae are pelagic, living in the water column for days to months before they settle (Leis 1991). This pelagic stage facilitates the movement of individuals among spatially isolated populations (population connectivity), though multiple factors may contribute to the realized dispersal of larvae from their population of origin. Traditionally, it has been assumed that the most important of these is the pelagic larval duration (PLD) (Riginos and Victor 2001; Selkoe and Toonen 2011; Luiz et al. 2013), where a short PLD results in larval settlement close to the natal habitat with increased population differentiation over fine scales (Planes et al. 2001), and a long PLD allows for long-distance larval dispersal with reduced population differentiation. It is increasingly recognized that while PLD may influence larval dispersal, realized dispersal should be mediated by both complex and dynamic oceanographic features. Simulations have shown that even modest abilities for larvae to modulate their position in the water column can obscure the relationship between PLD, oceanographic features, and realized larval dispersal (Cowen et al. 2006; Leis 2007). Indeed, larval dispersal of marine species is most likely modulated by some combination of PLD, oceanographic features, and larval behavior, as well as environmental factors such as temperature and food availability.

In this study, we brought together the necessity for understanding the level of connectivity in the Mozambique Channel (Western Indian Ocean), and the use of genetic techniques on two coral reef damselfish (family Pomacentridae), the three-spot dascyllus, *Dascyllus trimaculatus*, and the skunk clownfish, *Amphiprion akallopisos*. The two species exhibit differences in both PLD and habitat use. Reported PLD ranges from 7 to 22 d for *Amphiprion* species and from 20 to 30 d for *D. trimaculatus* (Thresher et al. 1989; Wellington and Victor 1989; Robitzsch et al. 2015). Both species are symbiotic mutualists of sessile sea anemones as juveniles. As subadults, however, while clownfish remain with their host, *D. trimaculatus* leave the

anemones altogether to feed on plankton in the water column (Fautin and Allen 1997), which may increase the potential number of lifetime mates and thus the probability of mating events with individuals from distant populations that increase genetic homogeneity. Clownfish larval dispersal distances have been shown to vary from <1 km (Beldade et al. 2012; Saenz-Agudelo et al. 2012) to >100 km (Simpson et al. 2014). However, despite only small differences in PLDs compared to clownfishes, *D. trimaculatus* have been shown to have large-scale genetic homogeneity, spanning >1000 km (Bernardi et al. 2001, 2002, 2003; Leray et al. 2010).

The Mozambique Channel is an arm of the Western Indian Ocean spanning approximately 500 km between Mozambique and Madagascar and 1200 km between its limits to the north (the Comoros Islands) and south (the southern end of Madagascar). A string of four oceanic island groups runs along its center from north to south: Îles Glorieuses (an archipelago of two nearby islands, Grande Glorieuse and Île du Lys), Juan de Nova, Bassas da India, and Europa (Fig. 1). These islands, together with the island of Tromelin, which lies outside of the Mozambique Channel to the east of Madagascar, make up the Îles Éparses (English translation: Scattered Islands), an overseas administrative division of France. They harbor moderate levels of coral reef biodiversity (Fricke et al. 2013) and are relatively pristine because there are no permanent

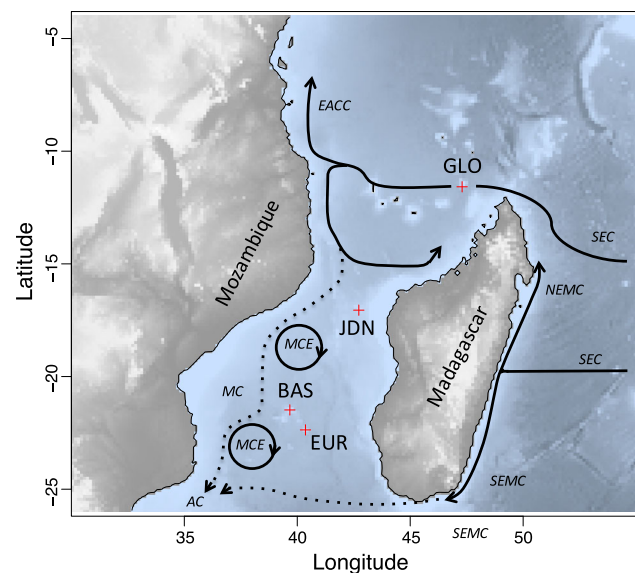


**Fig. 1** Location of collection sites in the Mozambique Channel (GLO: Îles Glorieuses, JDN: Juan de Nova, BAS: Bassas da India, EUR: Europa). Main currents and flow features are shown: South Equatorial Current (SEC), the Northeast and Southeast Madagascar Currents (NEMC and SEMC), the East African Coastal Current (EACC), the Agulhas Current (AC), the Mozambique Current (MC), and the Mozambique Channel Eddies (MCE). Poorly documented currents are presented with dashed lines (Redrawn from Schouten et al. 2003)

human settlements, making them primary candidates for marine conservation. Following the most recent biogeographic division of this area's eco-regions (Spalding et al. 2007; Obura 2012), the southern Europa, Bassas da India, and Juan de Nova islands are separate from the northern Îles Glorieuses. These islands provide habitat for coastal marine organisms close enough for potential migration via larval dispersal, but distant enough to prevent adult dispersal. The optimal strategy for marine conservation of the Scattered Islands depends on the degree of population connectivity among them, making it important to know whether or not population structure follows the same pattern as community structure.

In this region, the oceanographic circulation patterns have been relatively better studied than genetic connectivity of coral reef fishes. The Mozambique Channel lies in the shadow of the South Equatorial Current (Fig. 1). Strong eddies form approximately four times per year following cyclonic and anticyclonic directions (Schouten et al. 2003; Lutjeharms and Bornman 2010; Swart et al. 2010; Lutjeharms et al. 2012). Though the sites included in our study are small and isolated, these eddies may serve to enhance larval retention, restricting connectivity and therefore potentially increasing genetic structure among sites. In this region, changes in local ocean circulation may take place over timescales from seasonal to decadal (Schouten et al. 2003; Lutjeharms et al. 2012) adding another element of stochasticity in the prediction of population structure between the islands in the channel.

Very few studies have examined population connectivity of coral reef fishes in the Mozambique Channel. For the bluestripe snapper, *Lutjanus kasmira*, the blotcheye soldierfish, *Myripristis berndti*, and the honeycomb grouper, *Epinephelus merra*, while population structure was found at the level of the Western Indian Ocean, no population structure was found within the Mozambique Channel (Muths et al. 2011, 2012, 2015). In this study, we used microsatellite markers to assess the level of connectivity exhibited by *A. akallopisos* and *D. trimaculatus* that were collected at all four of the Scattered Islands groups of the Mozambique Channel. We tested models of genetic structure and migration among the four Scattered Islands in light of the previously identified divide in eco-regions and the presence and location of known eddies as potential barriers to gene flow.

## Methods

### Sample collection

Adult and subadult fish were collected at all four island groups in the Mozambique Channel: Îles Glorieuses

(GLO), Juan de Nova (JDN), Bassas da India (BAS), and Europa (EUR; Fig. 1). Individuals were captured using hand nets, and a small piece of fin tissue was collected before returning fish to their host anemone. Tissue samples were placed in 95% ethanol and stored at  $-20^{\circ}\text{C}$  as soon as possible.

### Laboratory methods

Genomic DNA was extracted using a chloroform-based protocol (Sambrook et al. 1989). Microsatellite loci were originally isolated and developed for *Amphiprion chrysopterus* and *Amphiprion polymnus* (Quenouille et al. 2004; Beldade et al. 2009) and for *D. trimaculatus* (Leray et al. 2008). From the existing libraries, we chose 20 microsatellites per species to test for variability on 32 individuals. Nine polymorphic loci for *A. akallopisos* and 13 for *D. trimaculatus* were selected based on their variability and amplification success rate (Table 1). Each reaction contained 5  $\mu\text{l}$  of Qiagen Multiplex PCR master-mix, 0.2 pmol of each primer, and 0.8  $\mu\text{l}$  of DNA diluted with RNAase-free water to a total reaction volume of 10  $\mu\text{l}$ . The following temperature profile was used: 15 min at  $95^{\circ}\text{C}$ , followed by 40 cycles of 30 s at  $94^{\circ}\text{C}$ , 1 min and 30 s at  $57^{\circ}\text{C}$ , and 1 min at  $72^{\circ}\text{C}$ , with a final extension of 7 min at  $72^{\circ}\text{C}$ . PCR product was diluted with 50  $\mu\text{l}$  of water, and 0.5  $\mu\text{l}$  of this diluted PCR product was added to 9.74  $\mu\text{l}$  of HiDi formamide and 0.26  $\mu\text{l}$  ROX 500 size standard (Qiagen, Valencia, California). Fragment size was analyzed on an ABI 96 capillary 3730XL DNA Analyzer (Applied Biosystems, Darmstadt, Germany).

### Data analysis

We genotyped individuals using GeneMapper version 3.7 (Applied Biosystems), and Convert v1.31 (Glaubitz 2004) was used to generate input files for various analyses programs. We checked for null alleles and scoring errors using Micro-checker v.2.2.3 (Van Oosterhout et al. 2004). Arlequin v3.11 (Excoffier et al. 2005) was used to calculate expected and observed heterozygosities, test for deviation from Hardy–Weinberg Equilibrium (HWE) using a Markov chain of length 100,000, and test for linkage disequilibrium. Using Weir and Cockerham (1984) formulae, we calculated  $F_{IS}$  using the function  $f_{st}$  in the R package pegas version 0.9 (Paradis 2010; R core Team 2015) and calculated global significance values using Goudet's  $G$  statistic Monte Carlo test on 1000 iterations with the function  $gstat.randtest$  in the R package hierfstat version 0.04–22 (Goudet and Jombart 2015; R Core Team 2015). Several measures of genetic structure were used, including  $F_{ST}$  and  $R_{ST}$  implemented in Arlequin v3.11, and  $G'_{ST}$  and Jost's  $D$  implemented in the R package diveRsity (Keenan et al.

**Table 1** Summaries of the microsatellite loci used in this study. Number of alleles (Na) and fragment lengths (RR, given in base pairs) for microsatellite loci used in this study for *Amphiprion akallopisos* (top panel) and *Dascyllus trimaculatus* (bottom panel), as well as number of alleles (Na), observed (Ho) and expected (He) heterozygosities for each locus at each sampled site

| <i>A. akallopisos</i>  |    |         |                                  |       |       |                               |       |       |                                |       |       |       |         |
|------------------------|----|---------|----------------------------------|-------|-------|-------------------------------|-------|-------|--------------------------------|-------|-------|-------|---------|
| Locus                  | Na | RR (bp) | Îles Glorieuses ( <i>n</i> = 31) |       |       | Juan de Nova ( <i>n</i> = 37) |       |       | Europa–Bassas ( <i>n</i> = 41) |       |       | Total |         |
|                        |    |         | Na                               | Ho    | He    | Na                            | Ho    | He    | Na                             | Ho    | He    | % NA  | FIS     |
| B6                     | 8  | 141–159 | 5                                | 0.781 | 0.691 | 8                             | 0.757 | 0.746 | 6                              | 0.829 | 0.686 | 0     | –0.120* |
| D114                   | 6  | 202–222 | 4                                | 0.613 | 0.632 | 5                             | 0.621 | 0.639 | 5                              | 0.732 | 0.675 | 0.9   | –0.006* |
| 44                     | 11 | 241–256 | 8                                | 0.548 | 0.728 | 6                             | 0.5   | 0.673 | 5                              | 0.548 | 0.606 | 10.9  | 0.249*  |
| 34                     | 34 | 296–359 | 21                               | 0.844 | 0.885 | 19                            | 0.703 | 0.871 | 19                             | 0.829 | 0.881 | 0     | 0.098*  |
| 120                    | 2  | 454–456 | 2                                | 0.375 | 0.347 | 2                             | 0.216 | 0.195 | 2                              | 0.146 | 0.217 | 0     | 0.039   |
| D103                   | 15 | 250–306 | 13                               | 0.969 | 0.887 | 11                            | 0.811 | 0.882 | 11                             | 0.829 | 0.888 | 0     | 0.026*  |
| CF11                   | 19 | 184–214 | 10                               | 0.774 | 0.714 | 13                            | 0.838 | 0.792 | 11                             | 0.78  | 0.702 | 0.9   | –0.081  |
| 10TCTA                 | 35 | 500–558 | 26                               | 1     | 0.937 | 20                            | 0.914 | 0.891 | 19                             | 0.846 | 0.909 | 3.6   | –0.010* |
| A130                   | 15 | 171–194 | 9                                | 0.08  | 0.811 | 9                             | 0.194 | 0.49  | 10                             | 0.132 | 0.691 | 10    | 0.787*  |
| <i>D. trimaculatus</i> |    |         |                                  |       |       |                               |       |       |                                |       |       |       |         |
| Locus                  | Na | RR (bp) | Îles Glorieuses ( <i>n</i> = 45) |       |       | Juan de Nova ( <i>n</i> = 32) |       |       | Europa–Bassas ( <i>n</i> = 42) |       |       | Total |         |
|                        |    |         | Na                               | Ho    | He    | Na                            | Ho    | He    | Na                             | Ho    | He    | % NA  | FIS     |
| A7                     | 8  | 236–250 | 7                                | 0.689 | 0.77  | 8                             | 0.719 | 0.788 | 7                              | 0.61  | 0.658 | 0.8   | 0.097   |
| A101                   | 32 | 108–188 | 28                               | 0.8   | 0.965 | 24                            | 0.733 | 0.965 | 24                             | 0.707 | 0.947 | 2.5   | 0.222   |
| A103                   | 27 | 181–259 | 21                               | 0.689 | 0.945 | 20                            | 0.688 | 0.931 | 21                             | 0.561 | 0.937 | 0.8   | 0.315   |
| A105                   | 23 | 133–181 | 20                               | 0.889 | 0.926 | 17                            | 0.966 | 0.917 | 19                             | 0.853 | 0.918 | 0.8   | 0.251   |
| A111                   | 37 | 243–389 | 31                               | 0.578 | 0.967 | 24                            | 0.581 | 0.962 | 30                             | 0.548 | 0.963 | 0     | 0.033   |
| A114                   | 16 | 222–290 | 14                               | 0.644 | 0.916 | 14                            | 0.75  | 0.9   | 15                             | 0.675 | 0.885 | 1.7   | 0.348   |
| A115                   | 21 | 165–251 | 19                               | 0.262 | 0.916 | 13                            | 0.16  | 0.891 | 14                             | 0.313 | 0.909 | 3.4   | 0.028   |
| A120                   | 24 | 164–222 | 19                               | 0.778 | 0.93  | 19                            | 0.71  | 0.911 | 18                             | 0.595 | 0.918 | 6.7   | 0.151   |
| B103                   | 15 | 280–308 | 11                               | 0.889 | 0.879 | 13                            | 0.844 | 0.889 | 14                             | 0.833 | 0.888 | 0.8   | 0.413   |
| B105                   | 29 | 173–251 | 25                               | 0.711 | 0.956 | 17                            | 0.531 | 0.884 | 18                             | 0.55  | 0.918 | 1.7   | 0.247   |
| B109                   | 30 | 184–256 | 27                               | 0.778 | 0.941 | 21                            | 0.929 | 0.927 | 20                             | 0.737 | 0.944 | 5     | 0.36    |
| B113                   | 28 | 226–316 | 24                               | 0.738 | 0.948 | 16                            | 0.5   | 0.906 | 20                             | 0.512 | 0.914 | 0     | 0.12    |
| C12                    | 9  | 251–315 | 8                                | 0.289 | 0.32  | 5                             | 0.281 | 0.306 | 5                              | 0.214 | 0.26  | 16.8  | 0.729   |

Sample sizes are given next to each site name. For each locus across sites, percent missing data (% NA) and  $F_{IS}$  values are given, with significance of a global Goudet's  $G$  statistic Monte Carlo test indicated with an asterisk (\*)

2013). Arlequin was also used to calculate the significance of  $F_{ST}$  values based on 1000 permutations. Since individuals were collected in anemones, where sibling individuals have been shown to occasionally co-recruit (Bernardi et al. 2012), we also tested for kinship of individuals (Loiselle et al. 1995) implemented in GENODIVE (Meirmans and Van Tienderen 2004), with a conservative cutoff value for full siblings at  $k > 0.4$ .

As an alternative approach to describing the genetic structure of the two pomacentrids, Bayesian clustering analyses were conducted using the software STRUCTURE (version 2.3) (Pritchard et al. 2000) and GENELAND v.4.0.3 (Guillot et al. 2005a, b). STRUCTURE implements a Markov chain Monte Carlo (MCMC) simulation approach to estimate the posterior probability that a sampled individual

belongs to each of  $K$  clusters based on its multi-locus genotype. We conducted analyses for values of  $K$  from 1 to 10, each consisting of 20 independent runs of MCMC length 1,000,000. The first 10,000 iterations of each chain were discarded as burn-in. We calculated an optimal value of  $K$  using the method described by Evanno et al. (2005) implemented by STRUCTURE HARVESTER (Earl and vonHoldt 2012); however, because a strict abiding of such results has recently been questioned (Meirmans 2015), we also present the results under alternate scenarios of  $K$ . GENELAND uses a model similar to STRUCTURE, but allows inclusion of the samples' geographic positions as a prior in the analysis in order to assess the posterior probability of cluster membership not only for individuals, but for each cell of a spatial grid, thus identifying geographic boundaries



between the identified clusters. Ten MCMC runs were conducted, each including 1,000,000 iterations with a thinning of 1000, based on the uncorrelated frequency model with no uncertainty of the sample coordinates, and where the number of clusters ( $K$ ) was allowed to vary between 1 and 4, based on the STRUCTURE output. Excluding the first 200 values out of the 1000 saved iterations as a burn-in, MCMC convergence was assessed by comparing the number of clusters across replicate runs, with a single run chosen for presentation on the basis of the mean posterior probability used as a criterion to choose the best run.

Finally, we used a discriminant analysis of principal components (DAPC) procedure described by Jombart et al. (2010) as an independent method for identifying the number of clusters ( $K$ ) and the probability of individual membership to each cluster. Briefly, we transformed the allele size data using principal component analysis, performed successive  $K$  means clustering (for  $K = 1–10$ ) on the transformed data retaining all principal components, and calculated the Bayesian information criterion (BIC) of each  $K$ . We chose an optimal value of  $K$  using Ward's hierarchical agglomerative clustering method on the differences in BIC between successive steps. Values were assigned to one of two groups representing large or small differences, and the value of  $K$  just before the first group switch was chosen as the optimum. Because the method for choice of an optimal  $K$  is debated, especially in the present context where groups are in reality not completely distinct, we also evaluated  $K$  based on the value at which a LOWESS curve began increasing, as well as the raw minimum BIC. If the optimum  $K$  was greater than 1, we evaluated the probability of membership to each cluster using discriminant function analysis. These operations were performed using the functions `find.clusters` and `dapc` in the R package `adegenet` version 2.0.1 (Jombart 2008).

## Results

### Microsatellite analysis

We successfully amplified nine microsatellite loci from 110 *A. akallopisos* and 13 microsatellites for 119 *D. trimaculatus* from four sites in the Mozambique Channel (Table 1; Fig. 1). Loci used in this study showed sufficient variability for a population study (2–37 alleles, mean = 20.2, SD = 10.4). Within sites, for *D. trimaculatus*, there was evidence of significant deviation from HWE in seven cases, but no site or microsatellite showed consistent deviation from HWE across populations, indicating that all sites and microsatellite loci were usable for this analysis. Kinship analysis identified two *A. akallopisos* individuals from Îles Glorieuses as being full siblings

( $R = 0.617$ ). Therefore, one individual from the pair was removed from the subsequent analyses. No other full-sib relationships were detected (not shown).

### Population structure of *D. trimaculatus* and *A. akallopisos*

Values of population differentiation were always greater in *A. akallopisos* than in *D. trimaculatus* (Table 2). Indeed, average population pairwise comparisons were higher in *A. akallopisos* than in *D. trimaculatus* for all metrics used in this study:  $F_{ST}$  (0.09 vs. 0.003),  $R_{ST}$  (0.08 vs. 0.00),  $G'_{ST}$  (0.03 vs. 0.00), and Jost's  $D$  (0.07 vs. 0.02). For *A. akallopisos*, while pairwise  $F_{ST}$  values were relatively low (<0.05), all three comparisons were found to be statistically significant (Table 2). In addition, for *A. akallopisos*, the Juan de Nova population was always most distinct from the two other populations (Table 2).

Both of the Bayesian clustering approaches were consistent with the classical population structure analyses presented above. Indeed, both indicated clear population structure in *A. akallopisos*, and less so for *D. trimaculatus*. The Evanno method identified two and four STRUCTURE clusters for *D. trimaculatus* and *A. akallopisos*,

**Table 2** Classical fixation indices among study sites. Pairwise  $F_{ST}$ ,  $R_{ST}$ ,  $G'_{ST}$ , and Jost's  $D$  values for sites sampled in this study

|                 | Îles Glorieuses | Juan de Nova | Europa–Bassas |
|-----------------|-----------------|--------------|---------------|
| $F_{ST}$        |                 |              |               |
| Îles Glorieuses | –               | 0.047*       | 0.033*        |
| Juan de Nova    | 0.001           | –            | 0.014*        |
| Europa–Bassas   | 0.001           | 0.006        | –             |
| $R_{ST}$        |                 |              |               |
| Îles Glorieuses | –               | 0.032*       | –0.004        |
| Juan de Nova    | 0.013           | –            | 0.031*        |
| Europa–Bassas   | 0.026           | 0.074*       | –             |
| $G'_{ST}$       |                 |              |               |
| Îles Glorieuses | –               | 0.031*       | 0.016*        |
| Juan de Nova    | 0.01            | –            | 0.023*        |
| Europa–Bassas   | 0.008           | 0.013        | –             |
| Jost's $D$      |                 |              |               |
| Îles Glorieuses | –               | 0.112*       | 0.056         |
| Juan de Nova    | 0.121           | –            | 0.079*        |
| Europa–Bassas   | 0.105           | 0.141        | –             |

Values for *Amphiprion akallopisos* italicized above the diagonal, values for *Dascyllus trimaculatus* are below the diagonal. For  $F_{ST}$  and  $R_{ST}$  values, asterisks indicate significance ( $p < 0.05$ ) based on 100 permutations computed in ARLEQUIN v3.1 (Excoffier et al. 2005). Values for  $G'_{ST}$  and Jost's  $D$  were calculated using the R package `diveRsity` (Keenan et al. 2013), and asterisks indicate estimates for which the 95% confidence interval does not contain zero

respectively (Electronic Supplementary Materials, ESM, Fig. 1). Results with no structure at all ( $K = 1$ ) for *D. trimaculatus* were not significantly different than the chosen ones ( $K = 2$ ) thus being consistent with the classical population genetics approach. Finally, for easier comparative visualization, Evanno's method results ( $K = 2$  and  $K = 4$ ) and keeping clusters at three ( $K = 3$ ) for both species are presented in Fig. 2. This visualization illustrates the clear difference between the two species; *A. akallopisos* show stronger population structure than *D. trimaculatus*. In addition, as for the classical population genetic approach, the Juan de Nova *A. akallopisos* population was most different from the two other populations (Fig. 2).

GENELAND's spatially explicit algorithm also clearly showed a difference between the two species. While it only identified a single panmictic population for *D. trimaculatus*, three clusters were identified for *A. akallopisos*. GENELAND specifically assigned those clusters to the three regions sampled here (north, central, and south Mozambique Channel), with the geographically close Bassas da India and Europa grouped together (Fig. 3). The accuracy of classification of spatial grid cells to genetic clusters is highest when the spatial origins of individual samples are

dense and uniformly distributed over the area of interest. Our samples were collected from only four sites over a very large area, making the boundaries of genetic clusters unlikely to be truly representative of the distribution of our study species' larvae in the ocean. Nevertheless, the analysis of GENELAND provides a useful visualization of the genetic clusters in space and provides a baseline against which to test genetic breaks in future studies. We present the results after removal of individuals for which no data were available for at least one locus. A preliminary analysis using individuals with missing data (not shown) yielded qualitatively similar results, but did not appropriately sample the cluster parameter or establish convergence after multiple runs.

The results of DAPC (ESM, Figs. 2, 3) are largely consistent with those of the Bayesian clustering algorithms implemented by STRUCTURE and GENELAND. For *D. trimaculatus*, BIC increased monotonically from  $K = 1$  to  $K = 10$ ; that is, the analysis was unable to identify any distinct groups from the data. For *A. akallopisos*, the value of BIC declined sharply from  $K = 1$  to  $K = 2$ , but remained very similar for  $K = 2-4$ . While a clustering-based approach identified  $K = 2$  to be optimal, the LOWESS and minimum BIC approaches suggest an

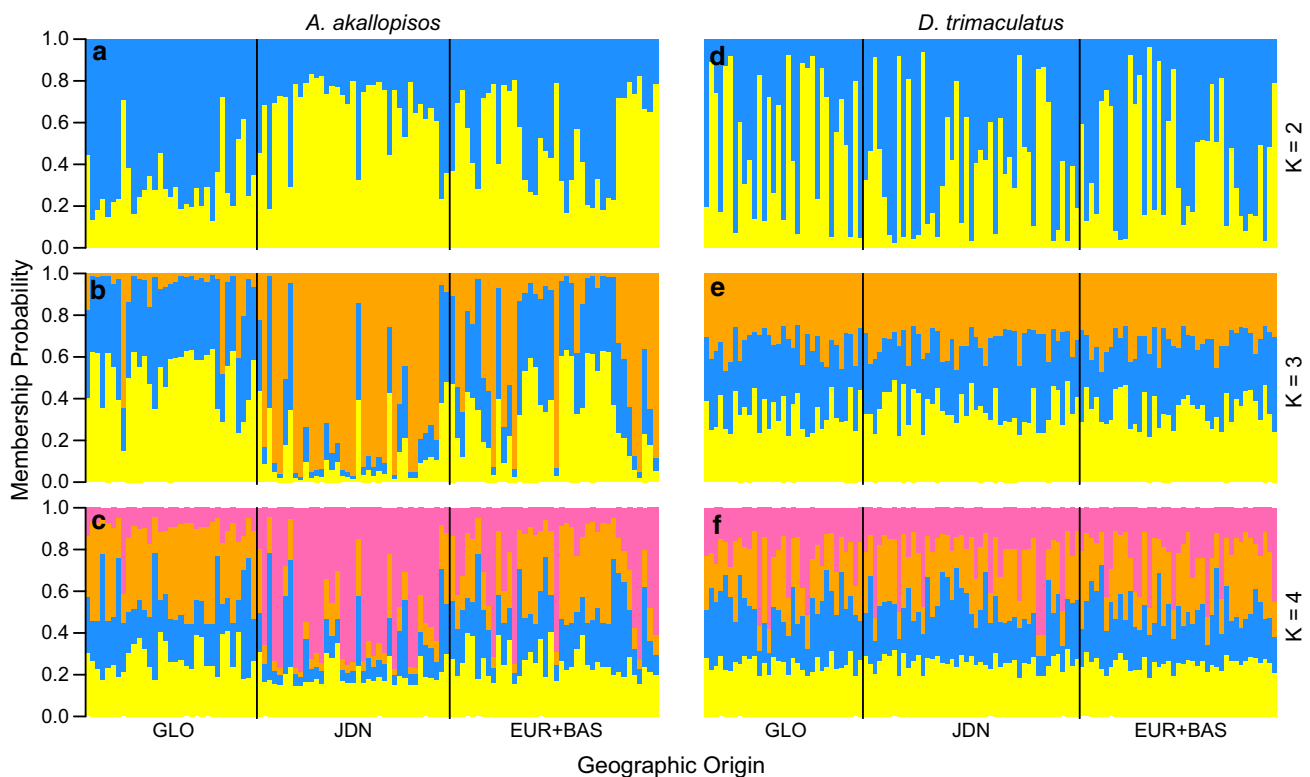


**Fig. 2** Plots representing output of Bayesian clustering algorithm implemented by STRUCTURE for *Amphiprion akallopisos* (a, b, c) and *Dascyllus trimaculatus* (d, e, f). Each vertical bar represents an individual, and the colors represent the posterior probability of its

membership to each cluster. The number of clusters selected ( $K = 2, 3$ , and 4) is indicated to the right. Populations are separated by black vertical bars as Îles Glorieuses (GLO), Juan de Nova (JDN), and Europa + Bassas da India (EUR + BAS)

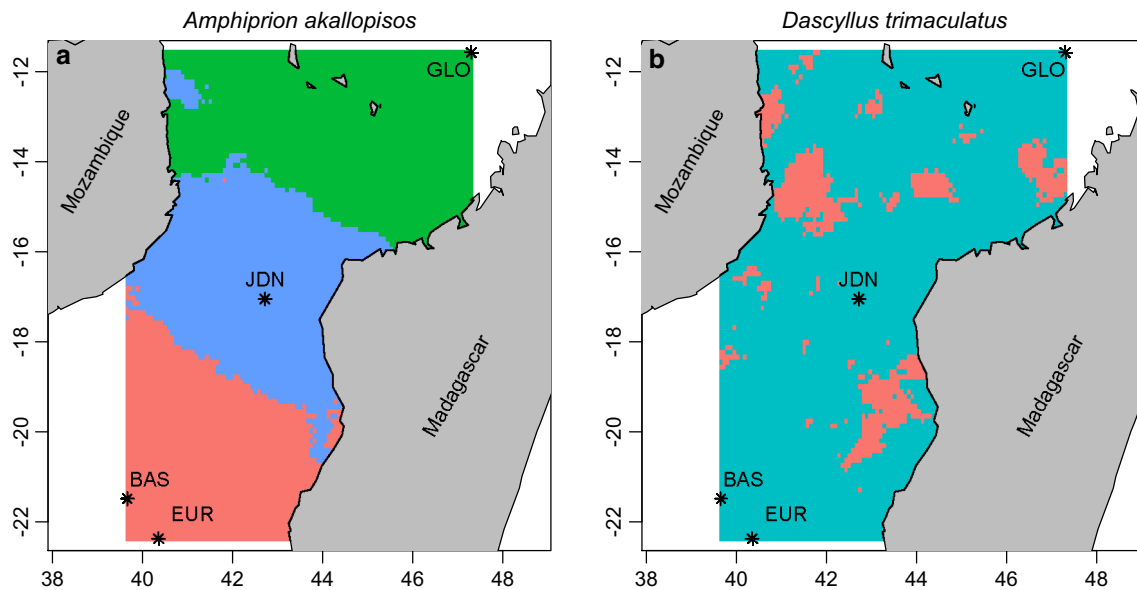


**Fig. 3** Maps representing the output of GENELAND for *A. akallopisos* (a) and *D. trimaculatus* (b). The 100 by 100 grid cells are colored by modal estimated cluster membership based on posterior probabilities of 1 million iterations. This represents the dataset after removal of

individuals for which no data were available for at least one locus. A preliminary analysis using individuals with missing data (not shown) yielded qualitatively similar results, but did not appropriately sample the cluster parameter or establish convergence after multiple runs

optimum  $K$  of 3 and 4, respectively. DAPC assigned nearly all individuals to one of the genetic clusters with almost complete certainty, while the Bayesian approaches generally split the uncertainty when the number of clusters was greater than the most likely, as expected.

## Discussion

We found discordant patterns of population connectivity between two damselfish species that, while closely related, differ in strategies at both the larval and adult stage. Notably, the pattern of genetic structure over our study's scale differs from a prediction of simple isolation by distance and from previously defined eco-regions yet resemble the patterns from other fish species in the area.

### Population structure patterns

While we found no evidence of genetic structure among any of the Îles Éparses for *D. trimaculatus*, the species with the longest PLD, low levels of genetic structure were revealed in *A. akallopisos* based on any and all metrics used in this study. These results were consistent using metrics of population differentiation ( $F_{ST}$ ,  $R_{ST}$ ,  $G'_{ST}$ , and Jost  $D$ ), as well as Bayesian clustering analyses.

The shorter PLD (7–22 d) and more restricted adult movement of *A. akallopisos* adults might have played a determinant role in the genetic differentiation found across islands. Our results for *D. trimaculatus* with a longer PLD

are also consistent with the lack of structure found in species from previous studies. Indeed, *D. trimaculatus* exhibits a PLD (20–30 d) that is similar or shorter than the three other species studied in the region, *L. kasmira* (30 d), *E. merra* (30 d), and *M. berndti* (55 d) (Muths et al. 2011, 2012, 2015). These three species are broadcast spawners, with both eggs and larvae being pelagic, while both species included in our study are benthic spawners (laying eggs directly on the substrate, like all pomacentrids) with pelagic larvae. While egg type and nesting strategy have been evoked to predict population structure in marine fishes, our results do not indicate a significant difference in structure between the broadcast spawners *L. kasmira*, *E. merra*, and *M. berndti* and the benthic spawning *D. trimaculatus* with a similar PLD.

Similar to our results for *A. akallopisos*, higher  $F_{ST}$  values between Îles Glorieuses and Juan de Nova compared to those between Îles Glorieuses and Europa were reported for the soldierfish *M. berndti* (Muths et al. 2011). This pattern contrasts with the eco-regions proposed by Spalding et al. (2007) and reviewed by Obura (2012). These regions are delimited on the basis of differences in community composition driven by taxonomic turnover at or above the species level, implicating a barrier that creates or maintains the range limit of many taxa. Other species' ranges span such boundaries, but may or may not exhibit genetic differentiation. A lack of population genetic differentiation across eco-regions indicates that the forces driving population connectivity differ from those responsible for community-level patterns. Studies of such cases

can help identify the processes that are important in maintaining diversity across and within spatially isolated communities. But perhaps even more interesting than the lack of concordance with eco-regions is that individuals from a site situated between the others (Juan de Nova) are assigned to a different genetic cluster than those on either side.

### Oceanography and connectivity

One factor that may explain this unusual pattern of disjunct genetic structure is the complex oceanographic features of the region (see Fig. 1 in Schouten et al. 2003), which will influence the fate of the migrating larvae between the islands. The Mozambique Channel lies in the shadow of the south equatorial current, and while previously thought to be dominated by the southward flowing Mozambique Current (Sætre 1985), it has now been shown that strong eddies form within the channel approximately four times per year (Schouten et al. 2003). Though the sites included in our study are small and isolated, these eddies may serve to enhance self-recruitment, especially for species with short PLDs, and therefore increase genetic structure among sites. Oceanographic features such as seasonal eddies have been shown to drive genetic connectivity of reef fishes elsewhere (e.g., Beldade et al. 2014). The eddies in the narrowest part of the Mozambique Channel near Juan de Nova may increase retention rates of larvae with short durations, such as *A. akallopisos*. Both species in this study are known to spawn approximately twice per lunar cycle, increasing the likelihood that larvae are distributed during periods of both eddy presence and absence.

The Scattered Islands are conservation priorities because of their species richness, isolation, and very low anthropogenic pressure. The present study and recent work in this region encompassing a total of five coral reef fish species with different life history traits (free or attached eggs, duration of the PLD, mobility as adults, life span, fecundity, etc.) will inform conservation and management plans for this region. The contrasting patterns of genetic structure and connectivity found for *M. berndti* and *A. akallopisos* showing a shallow level of genetic structure and weaker connectivity between Juan de Nova and the other Scattered islands, and *D. trimaculatus*, *L. kasmira*, and *E. merra* showing virtually no structure at this spatial scale, highlight the need for different strategies depending on the target species considered. Given the putative dispersal routes among the Îles Éparses, it would be very interesting to determine the origin of larvae in the descending current (along Mozambique) and the northward current (along Madagascar). The proximity and likely sharing of genetic material between species in the Scattered Islands, Mozambique, and Madagascar encourages the inclusion of

samples from sites on either side of the channel, as well as the comparison of these results to other species.

**Acknowledgments** Financial support was provided from INEE-INSU-IRD-AAMP-FRB-TAAF-Îles Éparses (Clownfish) to SCM and GB, Agence National de Recherche (ANR-11-JSV7-012-01/Live and Let Die) to SCM, LabEx “CORAIL” (“Where do we go now?”) to RB, FCT (SFRH/BPD/26901/2006) to RB, University of California Santa Cruz Department of Ecology and Evolutionary Biology (to JO) and Committee on Research (to GB), and Sigma Xi to JO. We would like to thank the administration of the TAAF (Terres australes et antarctiques françaises) for research permits and the captain and crew of the RV Marion Dufresne 2. For their assistance with the fieldwork, we wish to thank Pascale Chabanet, Lionel Bigot, Patrick Durville, and David Obura, as well as Jean-Bernard Galves and José Parodi of the RV Inventive. We are greatly appreciative of the constructive feedback given by the editor and three anonymous reviewers.

### References

- Allen GR (2008) Conservation hotspots of biodiversity and endemism for Indo-Pacific coral reef fishes. *Aquat Conserv* 18:541–556
- Beldade R, Holbrook SJ, Schmitt RJ, Planes S, Bernardi G (2009) Isolation and characterization of eight polymorphic microsatellite markers from the orange-fin anemonefish, *Amphiprion chrysopterus*. *Conserv Genet Resour* 1:333–335
- Beldade R, Jackson A, Cudney-Bueno R, Raimondi P, Bernardi G (2014) Genetic structure among spawning aggregations of the gulf coney *Hyporthodus acanthistius*. *Mar Ecol Prog Ser* 499:193–201
- Beldade R, Holbrook SJ, Schmitt RJ, Planes S, Malone D, Bernardi G (2012) Larger female fish contribute disproportionately more to self-replenishment. *Proc R Soc Lond B Biol Sci* 279:2116–2121
- Bernardi G, Holbrook SJ, Schmitt RJ (2001) Dispersal of the coral reef three-spot damselfish, *Dascyllus trimaculatus*, at three spatial scales. *Mar Biol* 138:457–465
- Bernardi G, Holbrook SJ, Schmitt RJ, Crane NL (2003) Genetic evidence for two distinct clades in a French Polynesian population of the coral reef three-spot damselfish *Dascyllus trimaculatus*. *Mar Biol* 143:485–490
- Bernardi G, Beldade R, Holbrook SJ, Schmitt RJ (2012) Full-sibs in cohorts of newly settled coral reef fishes. *PLoS One* 7:e44953
- Bernardi G, Holbrook SJ, Schmitt RJ, Crane NL, DeMartini E (2002) Species boundaries, populations, and colour morphs in the coral reef three-spot damselfish (*Dascyllus trimaculatus*) species-complex. *Proc R Soc Lond B Biol Sci* 269:599–605
- Briggs JC, Bowen BW (2012) A realignment of marine biogeographic provinces with particular reference to fish distributions. *J Biogeogr* 39:12–30
- Cowen RK, Paris CB, Srinivasan A (2006) Scaling of connectivity in marine populations. *Science* 311:522–527
- Earl DA, vonHoldt BM (2012) STRUCTURE HARVESTER: a website and program for visualizing STRUCTURE output and implementing the Evanno method. *Conserv Genet Resour* 4:359–361
- Evanno G, Regnaut S, Goudet J (2005) Detecting the number of clusters of individuals using the software STRUCTURE: a simulation study. *Mol Ecol* 14:2611–2620
- Excoffier L, Laval G, Schneider S (2005) Arlequin (version 3.0): an integrated software package for population genetics data analysis. *Evol Bioinform Online* 1:47–50
- Fautin DG, Allen GR (1997) Anemonefishes and their host sea anemones. Western Australian Museum, Perth, 167 pp



- Fricke R, Durville P, Bernardi G, Borsa P, Mou-Tham G, Chabanet P (2013) Checklist of the shore fishes of Europa Island, Mozambique Channel, southwestern Indian Ocean, including 302 new records. *Stuttgarter Beiträge zur Naturkunde A, Neue Serie* 6:247–276
- Glaubitz JC (2004) Convert: A user-friendly program to reformat diploid genotypic data for commonly used population genetic software packages. *Mol Ecol Notes* 4:309–310
- Goudet J, Jombart T (2015) hierfstat: Estimation and tests of hierarchical F-Statistics. R package version 0.04-22
- Guillot G, Mortier F, Estoup A (2005a) GENELAND: a computer package for landscape genetics. *Mol Ecol Notes* 5:712–715
- Guillot G, Estoup A, Mortier F, Cosson JF (2005b) A spatial statistical model for landscape genetics. *Genetics* 170:1261–1280
- Halpern BS, Warner RR (2003) Matching marine reserve design to reserve objectives. *Proc R Soc Lond B Biol Sci* 270:1871–1878
- Jombart T (2008) adegenet: an R package for the multivariate analysis of genetic markers. *Bioinformatics* 24:1403–1405
- Jombart T, Devillard S, Balloux F (2010) Discriminant analysis of principal components: a new method for the analysis of genetically structured populations. *BMC Genet* 11:94
- Keenan K, McGinnity P, Cross TF, Crozier WW, Prodöhl PA (2013) diveRcity: An R package for the estimation of population genetics parameters and their associated errors. *Methods Ecol Evol* 4:782–788
- Leis JM (1991) The pelagic stage of reef fishes: The larval biology of coral reef fishes. In: Sale, PF (ed) *The ecology of fishes on coral reefs*. pp 183–230
- Leis JM (2007) Behaviour as input for modelling dispersal of fish larvae: behaviour, biogeography, hydrodynamics, ontogeny, physiology and phylogeny meet hydrography. *Mar Ecol Prog Ser* 347:185–193
- Leray M, Beldade R, Holbrook S, Schmitt R, Planes S, Bernardi G (2008) Isolation and characterization of 13 polymorphic nuclear microsatellite primers for the widespread Indo-Pacific three-spot damselfish, *Dascyllus trimaculatus*, and closely related *D. auripinnis*. *Mol Ecol Resour* 9:213–215
- Leray M, Beldade R, Holbrook SJ, Schmitt RJ, Planes S, Bernardi G (2010) Speciation on coral reefs: vicariance and dispersal in the three-spot dascyllus, *Dascyllus trimaculatus*, species complex. *Evolution* 64:1218–1230
- Loiselle BA, Sork VL, Nason J, Graham C (1995) Spatial genetic-structure of a tropical understory shrub, *Psychotria officinalis* (Rubiaceae). *Am J Bot* 82:1420–1425
- Lutjeharms JRE, Bornman TG (2010) The importance of the greater Agulhas Current is increasingly being recognised. *S Afr J Sci* 106:1–4
- Lutjeharms JRE, Biastoch A, Van Der Werf PM, Ridderinkhof H, De Ruijter WPM, Town C, Africa S, Albrechts C, Burg D, Sciences M (2012) On the discontinuous nature of the Mozambique Current. *S Afr J Sci* 108:1–5
- Luiz OJ, Allen AP, Robertson DR, Floeter SR, Kulbicki M, Vigliola L, Becheler R, Madin JS (2013) Adult and larval traits as determinants of geographic range size among tropical reef fishes. *Proc Natl Acad Sci* 110:16498–16502
- McClanahan TR, Sheppard CRC, Obura DO (2000) *Coral reefs of the Indian Ocean: their ecology and conservation*. Oxford University Press, Oxford, 525 pp
- McClanahan TR, Ateweberhan M, Darling ES, Graham NAJ, Muthiga NA (2014) Biogeography and change among regional coral communities across the Western Indian Ocean. *PLoS One* 9:e93385
- Meirmans PG (2015) Seven common mistakes in population genetics and how to avoid them. *Mol Ecol* 24:3223–3231
- Meirmans PG, Van Tienderen PH (2004) GENOTYPE and GENODIVE: two programs for the analysis of genetic diversity of asexual organisms. *Mol Ecol Notes* 4:792–794
- Mills SC, Beldade R, Chabanet P, Bigot L, O'Donnell J, Bernardi G (2015) Ghosts of thermal past: reef fish exposed to historic high temperatures have heightened stress response to further stressors. *Coral Reefs* 34:1255–1260
- Mora C, Andréfouët S, Costello MJ, Kranenburg C, Rollo A, Veron J, Gaston KJ, Myers RA (2006) Coral Reefs and the global network of marine protected areas. *Science* 312:1750–1751
- Muths D, Tessier E, Bourjea J (2015) Genetic structure of the reef grouper *Epinephelus merra* in the West Indian Ocean appears congruent with biogeographic and oceanographic boundaries. *Mar Ecol* 36:447–461
- Muths D, Gouws G, Mwale M, Tessier E, Bourjea J, Moran P (2012) Genetic connectivity of the reef fish *Lutjanus kasmira* at the scale of the western Indian Ocean. *Can J Fish Aquat Sci* 69:842–853
- Muths D, Tessier E, Gouws G, Craig M, Mwale M, Mwaluma J, Mwandya A, Bourjea J (2011) Restricted dispersal of the reef fish *Myripristis berndti* at the scale of the SW Indian Ocean. *Mar Ecol Prog Ser* 443:167–180
- Obura D (2012) The diversity and biogeography of Western Indian ocean reef-building corals. *PLoS One* 7:e45013
- Obura D (2015) An Indian Ocean centre of origin revisited: Palaeogene and Neogene influences defining a biogeographic realm. *J Biogeogr* 43:229–242
- Paradis E (2010) pegas: an R package for population genetics with an integrated-modular approach. *Bioinformatics* 26:419–420
- Planes S, Doherty P, Bernardi G (2001) Unusual case of extreme genetic divergence in a marine fish, *Acanthochromis polyacanthus*, within the Great Barrier Reef and the Coral Sea. *Evolution* 55:2263–2273
- Pritchard JK, Stephens M, Donnelly P (2000) Inference of population structure using multilocus genotype data. *Genetics* 155:945–959
- Quenouille B, Bouchenak-Khelladi Y, Hervet C, Planes S (2004) Eleven microsatellite loci for the saddleback clownfish *Amphiprion polymnus*. *Mol Ecol Notes* 4:291–293
- R Core Team (2015) R: A language and environment for statistical computing. R Foundation for Statistical Computing, Vienna, Austria. <https://www.R-project.org/>
- Riginos C, Victor BC (2001) Larval spatial distributions and other early life-history characteristics predict genetic differentiation in eastern Pacific blennioid fishes. *Proc R Soc Lond B Biol Sci* 268:1931–1936
- Roberts CM, McClean CJ, Veron JEN, Hawkins JP, Allen GR, McAllister DE, Mittermeier CG, Schueler FW, Spalding M, Wells F, Vynne C, Werner TB (2002) Marine biodiversity hotspots and conservation priorities for tropical reefs. *Science* 295:1280–1284
- Robitzch VSN, Lozano-Cortés D, Kandler NM, Salas E, Berumen ML (2015) Productivity and sea surface temperature are correlated with the pelagic larval duration of damselfishes in the Red Sea. *Mar Pollut Bull* 105:566–574
- Saenz-Agudelo P, Jones GP, Thorrold SR (2012) Patterns and persistence of larval retention and connectivity in a marine fish metapopulation. *Mol Ecol* 21:4695–4705
- Sætre R (1985) Surface currents in the Mozambique Channel. *Deep Sea Res A* 32:1457–1467
- Sambrook J, Fritsch EF, Maniatis T (1989) *Molecular cloning: a laboratory manual*. Cold Spring Harbor Laboratory Press, Cold Spring Harbor, New York
- Schouten MW, Ruijter WPM, van Jan Leuwen P, Ridderinkhof H (2003) Eddies and variability in the Mozambique Channel. *Deep Sea Res Part II Top Stud Oceanogr* 50:1987–2003

- Selkoe KA, Toonen RJ (2011) Marine connectivity: a new look at pelagic larval duration and genetic metrics of dispersal. *Mar Ecol Prog Ser* 436:291–305
- Simpson SD, Harrison HB, Claereboudt MR, Planes S (2014) Long-distance dispersal via ocean currents connects Omani clownfish populations throughout entire species range. *PLoS One* 9:e107610
- Spalding MD, Fox HE, Allen GR, Davidson N, Ferdaña ZA, Finlayson M, Halpern BS, Jorge MA, Lombana A, Lourie SA, Martin KD, McManus E, Molnar J, Recchia CA, Robertson J (2007) Marine ecoregions of the world: a bioregionalization of coastal and shelf areas. *Bioscience* 57:573–583
- Swart NC, Lutjeharms JRE, Ridderinkhof H, Ruijter WPM (2010) Observed characteristics of Mozambique Channel eddies. *J Geophys Res* 115:C09006
- Thresher RE, Colin PL, Bell LJ (1989) Planktonic duration, distribution and population structure of western and central Pacific damselfishes (*Pomacentridae*). *Copeia* 2:420–434
- Van Oosterhout C, Hutchinson WF, Wills DPM, Shipley P (2004) MICRO-CHECKER: software for identifying and correcting genotyping errors in microsatellite data. *Mol Ecol Notes* 4:535–538
- Weir BS, Cockerham (1984) Estimating F-statistics for the analysis of population structure. *Evolution* 38:1358–1370
- Wellington GM, Victor BC (1989) Planktonic larval duration of one hundred species of Pacific and Atlantic damselfishes (*Pomacentridae*). *Mar Biol* 101:557–567